

Holocene evolution of deep circulation in the northern North Atlantic traced by Sm, Nd and Pb isotopes and bulk sediment mineralogy

N. Fagel¹ and N. Mattielli²

Received 11 May 2011; revised 30 September 2011; accepted 2 October 2011; published 14 December 2011.

[1] Bulk mineralogy, Sm, Nd and Pb elemental and isotopic compositions of the clay-size fraction of Holocene sediments were analyzed in three deep North Atlantic cores to trace the particle provenance. The aims of the present paper are to identify the origin of the particles driven by deep currents and to reconstruct deep circulation changes over the Holocene in the North Atlantic. The three cores are retrieved in fracture zones; two of them are located in the Iceland Basin along the gyre of North Atlantic Deep Water, and the third core is located off the present deep circulation gyre in the Labrador Sea. Whereas sedimentary supplies in the Labrador Sea were constantly derived from proximal sources, the geochemical mixing trends in the Iceland Basin samples indicate pronounced changes in the relative contribution of continental margin inputs over the past 6 kyr. Supplies from western European margin that sharply increased at 6 kyr were progressively diluted by a larger contribution of Scandinavian margins over the last 3 kyr. Changes in composition of the particles imply significant reorganization of paleocirculation of the deep North Atlantic components in the eastern basins: mainly reorganizations for both Iceland-Scotland Overflow Water and Norwegian Sea Overflow Water. Moreover the unusual Pb isotopic composition of the oldest sediments from the southern Iceland Basin indicates that distal supplies from Greenland margin were driven into the Iceland Basin, supporting a deep connection between Labrador Sea and Iceland Basin through the Charlie Gibbs Fracture Zone prior the Holocene Transition period.

Citation: Fagel, N., and N. Mattielli (2011), Holocene evolution of deep circulation in the northern North Atlantic traced by Sm, Nd and Pb isotopes and bulk sediment mineralogy, *Paleoceanography*, 26, PA4220, doi:10.1029/2011PA002168.

1. Introduction

[2] During the past decade many studies revealed the variability of deep ocean circulation over glacial/interglacial cycles. For instance variation in Nd isotope signatures measured in Fe-Mn nodules or sedimentary coatings have been interpreted in terms of North Atlantic Deep Water (NADW) export to the Southern Ocean [Rutberg *et al.*, 2000; Piotrowski *et al.*, 2005; Gutjahr *et al.*, 2010]. Instabilities in Holocene circulation and deep water production have increasingly been documented in marine archives [e.g., Bianchi and McCave, 1999; Oppo *et al.*, 2003; Andersen *et al.*, 2004a; Hall *et al.*, 2004]. Unstable deep-water conditions prior to the mid-Holocene optimum were mainly attributed to remnants of ice sheets [Bianchi and McCave, 1999]. However, the millennial variability in Atlantic circulation continued after the melting of the ice sheets [Andersen *et al.*, 2004a; Berner *et al.*, 2008]. In Subpolar North Atlantic

shifts in carbon isotope signatures of benthic forams provide evidence for 4 periods of reduced NADW contribution during the last 10 kyr [Oppo *et al.*, 2003]. The correlation between observed NADW disturbances [Bianchi and McCave, 1999; Oppo *et al.*, 2003; Hall *et al.*, 2004] and surface cooling events in Nordic Seas [Andersen *et al.*, 2004a; Berner *et al.*, 2008] argued for a linkage between surface variability and deep water masses over the Holocene [e.g., Giraudeau *et al.*, 2004, 2010].

[3] Radiogenic isotopes, and Nd in particular, have been used as a proxy for past deep circulation [e.g., van der Flierdt and Frank, 2010]. Most of the studies have focused on the water isotope signatures extracted from authigenic Fe-Mn nodules [Rutberg *et al.*, 2000; Frank, 2002; Gutjahr *et al.*, 2007], benthic foraminifera [Palmer and Elderfield, 1985; Vance *et al.*, 2004], fish teeth [Martin and Haley, 2000] and more recently in cold water corals [Colin *et al.*, 2010; Copard *et al.*, 2010; van der Flierdt and Frank, 2010]. Those proxies all record the isotopic signature of seawater that derives mainly from dissolution of continental inputs, exchange processes of seawater with particulates [Jeandel *et al.*, 1995] and interaction of seawater with sediments from continental margins [Lacan and Jeandel, 2005].

¹UR Argiles, Géochimie et Environnement Sédimentaires, Université de Liège, Liège, Belgium.

²Département des Sciences de la Terre et de l'Environnement, Université Libre de Bruxelles, Brussels, Belgium.

[4] Radiogenic isotopes of the detrital sedimentary fraction are used to trace sediment provenance [e.g., *McCulloch and Wasserburg*, 1978; *Jones et al.*, 1994; *Revel et al.*, 1996; *Walter et al.*, 2000; *Bayon et al.*, 2003], and the radiogenic isotope signature of continental detritus in the ocean can also be used as a proxy for deep circulation. In particular Sm, Nd and Pb isotope compositions constitute suitable tracers for the origin of deep sediments in the Labrador Sea [*Fagel et al.*, 1999, 2004]. The approach has been demonstrated over different timescales on several cores collected at a key site at the southern tip of Greenland: core HU90-013-017 [*Fagel et al.*, 1999], core MD99-2227 [*Fagel et al.*, 2002, 2004] and on the ODP Site 646 [*Fagel and Hillaire-Marcel*, 2006]. For instance changes in the Sm, Nd and Pb signatures of clay-size fraction of Late Glacial and Holocene sediments from core MD99-2227 provide constraints on the different source areas that supplied the fine clay-size particles into the Labrador Sea [*Fagel et al.*, 2004]. The sediment composition reflects variable contributions of mantle-derived distal sources from mid-Atlantic Ridge and crustal-derived proximal inputs from Canadian and Greenland margins. As distal inputs are only supplied by the deep current the isotopic composition of clay-size fraction of deep sediments record the fingerprint of the particles carried by the current. Radiogenic signatures can therefore be used as indirect paleoceanographic tracers. Changes in the relative contribution of the different sources deduced from geochemical mixing calculation provide information about the deep circulation pathways.

[5] The aim of this study is to document the changes in the contribution of the different components of the NADW in the Iceland and Labrador Sea basins over the Holocene. Bulk mineralogy and Sm, Nd and Pb isotopic compositions of three deep cores retrieved along the Bight and the Charlie-Gibbs fracture zones are combined to trace the sources of particulate supplies driven by deep currents. Geochemical mixing calculations are used to reconstruct the Holocene changes in the sedimentary supplies driven by the eastern components of the NADW. Our results will further be compared with previous investigations from Labrador Sea.

2. Material

[6] The sedimentological record of three deep drilling sites located in the northern North Atlantic basins, i.e., the Iceland Basin and the Labrador Sea were studied (Figure 1). Deep circulation in this area is, at present, under the influence of a contour-following current, the Western Boundary UnderCurrent (WBUC) [e.g., *McCartney*, 1992]. This current drives the components of the North Atlantic Deep Water masses, mainly the North East Atlantic Deep Water (NEADW), the Denmark Strait Overflow Water (DSOW) and the Davis Strait Overflow (DSO) in a counter-clockwise gyre from the southern tip of Greenland to the outlet of the Labrador Sea (Figure 1). The three studied cores were retrieved from fracture zones: cores MD99-2254 and HU91-045-080 mainly document the outflow from Norwegian Sea into the Iceland Basin whereas core HU91-045-091 lies below the modern pathway of the WBUC in the Labrador Sea. Our results will be compared with the isotopic data set from one core

recovered at the inlet of the WBUC pathway into the Labrador Sea (core MD99-2227, 3460 m water depth, southern tip off Greenland) [*Fagel et al.*, 2004].

[7] Core MD99-2254 was drilled from the Iceland Basin [*Turon et al.*, 1999]. The core was taken on the eastern flank of the Bight Fracture Zone at a water depth of 2440 m (56°47.78N, 30°39.86W, Figure 1). The site is bathed in the NEADW2 as defined by *Lucotte and Hillaire-Marcel* [1994]. The dominant lithologies are red to brown silty clays with foraminifers, with some bioturbation below 150 cm [*Turon et al.*, 1999]. The upper 140 cm of the core covers an interval spanning the Holocene and part of the late deglacial period, i.e., the last 18 kyr. The age model (Figure 2) was derived from 14 AMS ¹⁴C ages on planktonic foraminifera (Table S1).¹ The radiocarbon ages were corrected by a constant marine reservoir of 400 years and converted into calendar years using the Radiocarbon Calibration Program Calib 4.3 (<http://dept.washington.edu/qil/calib/calib.html>) [*Stuiver and Reimer*, 1993]). An age was assigned to each sample by assuming a linear sedimentation rate between two adjacent dates. All ages reported are calendar kyr BP and abbreviated as kyr. The 5 kyr time gap (from 8 to 13 kyr) between two adjacent radiocarbon dates suggests a pronounced hiatus between 80.5 and 86.5 cm. The upper core was subsampled with a 10 cm-resolution which represents a millennial time resolution. Twenty samples (0 to 190 cm) were analyzed for bulk mineralogy (Table S1) although in this study we report on the upper meter for Sm, Nd and Pb isotope compositions (11 samples; Table S4).

[8] Trigger weight HU91-045-080TWC and piston cores HU91-045-080P were retrieved in the Iceland Basin (Figure 1). The cores were drilled at 3024 m on the eastern side of the Charlie Gibbs Fracture Zone (53°03.40N, 33°31.78W [*Hillaire-Marcel et al.*, 1991]). The core is comprised of green to gray bioturbated clays [*Hillaire-Marcel et al.*, 1991]. The age model (Figure 2) is based on one radiocarbon date for TWC at 11.5 cm (0.78 kyr) and five radiocarbon dates for PC between 1 and 248 cm (from 5.3 to 17.2 kyr). Based on linear extrapolation of sedimentation rate, we estimate that the past 5 kyr are missing in the piston core, which corresponds to the upper 78 cm of the TWC. This correlation is in agreement with the lithological and mineralogical trends observed in TWC and PC cores (Figure 2). The most significant increase of the mean grain size (by ~2 microns) observed within the upper 10 cm of the piston core occurs between 75 and 85 cm in the trigger core. The upper increase of calcite (±10%) occurs most likely between 9 and 18 cm in piston core and between 85 and 95 cm in the trigger core. The cores were subsampled with a 10 cm-resolution: from 11.5 to 197 cm in TWC and from 1 to 248 cm in PC. Bulk mineralogy was analyzed on all the samples (Table S2). Isotopic analyses have been performed on the last 16 kyr with a sampling resolution averaging 500 years. Twenty-one samples have been analyzed: 9 from TWC and 12 from PC (Table S5).

[9] The core HU91-045-091 was taken in the deep Labrador Sea at a water depth of 3870 m (Figure 1). The

¹Auxiliary materials are available in the HTML. doi:10.1029/2011PA002168.

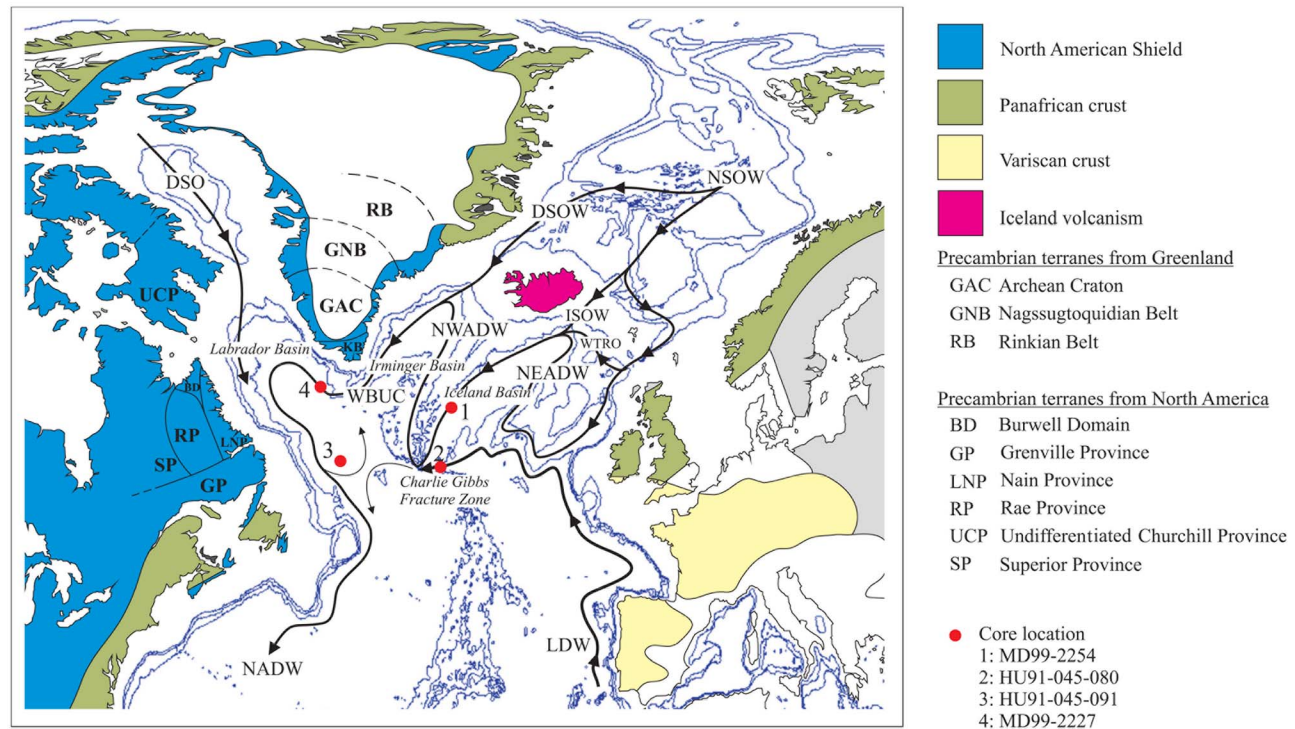


Figure 1. Location of sediment cores, deep current pathways and simplified geology of Northern North Atlantic margins (map modified from *Fagel et al.* [2004]). The arrows indicate the deep current pathways (modified from *McCartney* [1992], *Schmitz and McCartney* [1993], *Dickson and Brown* [1994], and *Lucotte and Hillaire-Marcel* [1994]). The structural terranes of the continental crusts (i.e., North American and Greenland Shield, Panafrican and Variscan crusts) adjacent to the northern North Atlantic (data from *Bridgewater et al.* [1991], *Kalsbeek et al.* [1993], and *Campbell et al.* [1996]) are indicated by different shades of gray levels. DSO, Davis Strait Overflow; DSOW, Denmark Strait Overflow Water; ISOW, Iceland-Scotland Overflow Water; LDW, Lower Deep Water; NEADW, North East Atlantic Deep Water; NWADW, North West Atlantic Deep Water; NADW, North Atlantic Deep Water; NSOW, Norwegian Sea Overflow Water; WBUC, Western Boundary UnderCurrent; WTRO, Wyville Thompson Ridge Overflow.

site is located at the western end of the Charlie Gibbs Fracture Zone (53°19.81N, 45°15.74W). The core is 45.5 cm long and consists of green olive to brown muds. Three lithological units have been identified [*Hillaire-Marcel et al.*, 1991], based on the occurrence of foraminifera (0–15 cm), silty layers (15 to 35 cm) and gravels in the lower part (35–45 cm). One radiocarbon date at 44 cm gives a calibrated age >18 kyr (15.500 yr ± 110). Additional stratigraphical information was derived from oxygen stable isotope measurements on *Neogloboquadrina pachyderma* (left coiled) foraminifers (Figure 2). The oxygen profile depicts a sharp shift at 39 cm. It is attributed to the Late Glacial/Holocene transition, in agreement with a 10% increase in the calcite abundance (Figure 2). The transition probably occurs close to the lithological change evidenced at 35 cm [*Hillaire-Marcel et al.*, 1991]. The cores were subsampled with a 0.5 to 1 cm-resolution. Bulk mineralogy was analyzed for the whole core (Table S3), and elemental Sm/Nd ratios and Pb isotopic compositions were analyzed on 17 Holocene samples between the surface and 29 cm (Table S6). In addition, we have also analyzed the Sm/Nd and Pb isotopic

signature of one Late Glacial sample, i.e., the deepest core interval (45–45, 5 cm; Table S6).

3. Method

3.1. Mineralogy

[10] In this study, bulk mineralogy may be indicative of particle provenance and it gives constraints on core stratigraphy. Bulk mineralogical compositions were identified by X-ray diffraction (XRD) using a Bruker D8-Advance diffractometer with CuK α radiation (ULg, Belgium). Sample powders were obtained by grinding ~1 g of dried <106 μ m fraction in a mortar. A powder mount was made using the back-side method [*Moore and Reynolds*, 1989]. XRD patterns have been recorded between 2 and 30°2 θ . Semiquantitative estimates of mineralogical composition were obtained by applying correction factors to the measured intensity of specific reflections for the main identified minerals [*Cook et al.*, 1975; *Boski et al.*, 1998]. The quartz intensity at 3.34 Å is taken as a reference ($I_{3.34} \times 1$). For K-feldspars, a factor of 4.3 is applied to the peak intensity comprised between 3.21 and 3.26 Å. For plagioclase, the

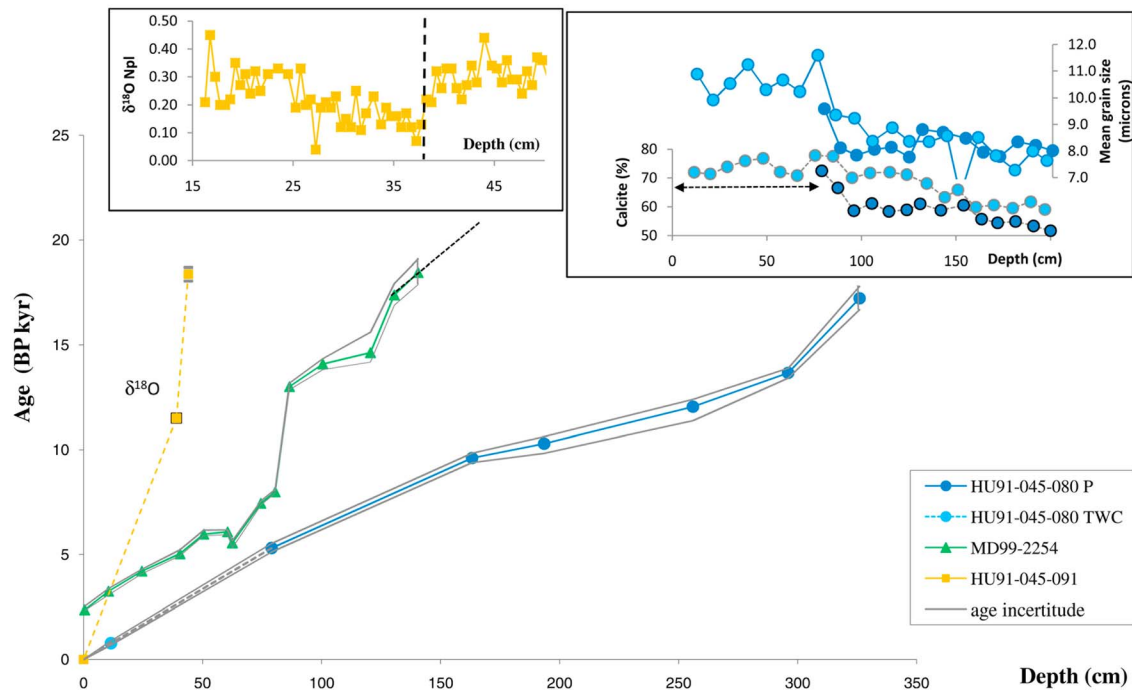


Figure 2. Age models of studied intervals for core HU91-045-091 (square); core HU91-045-080 (circle) and core MD99-2254 (triangle). Age model is mainly based on AMS14C dates measured on planktonic foraminifera assemblages, mainly on *Neogloboquadrina pachyderma* (left coiled) or on *Globigerina bulloides* (sample at 140.5 cm in core MD99-2254). Radiocarbon ages were converted to calibrated ages using CALIB 4.3 program [Stuiver and Reimer, 1993] and assuming a marine reservoir correction of -400 years. For site HU91-045-080 a composite core was made by adding the upper 78 cm of the trigger core (HU91-045-080TWC) to the piston core (HU91-045-080P). The correlation is consistent with lithological and mineralogical changes observed in both trigger and piston cores. Figure 2 (right) compares the abundance of calcite and the mean grain size in both cores: the profiles are parallel if the depths of the piston core are shifted by 78 cm. For core HU91-045-091 the age model is constrained by only two points: one radiocarbon date at 44 cm ($15500 \text{ yr} \pm 110$) and a shift in oxygen isotopic curve measured on *Neogloboquadrina pachyderma* (left coiled) foraminifers at 39 cm (Figure 2, left).

peak intensity at $3.16\text{--}3.21 \text{ \AA}$ is multiplied by 2.8. Pyroxene is identified by the peak at $2.98\text{--}3.00$ multiplied by 5. The peak at $8.27\text{--}8.59 \text{ \AA}$ is multiplied by 2.5 to estimate the amphibole. For calcite, the peak at $3.01\text{--}3.04 \text{ \AA}$ is multiplied by 1.65. Finally for the clay minerals, we take into account this common reflection at 4.47 \AA and we multiply its intensity by a factor of 20 in order to take into account their underestimation on bulk powder spectra [Boski et al., 1998]. Corrected intensities are summed to 100% and the relative abundance of each mineral group is calculated (Figure 3). Minerals are considered as *trace* when their abundance is lower than 2–3 wt.% (detection limit).

3.2. Geochemistry

[11] All concentrations and isotopic compositions were analyzed on the carbonate-free clay-size fraction ($<2 \mu\text{m}$). Samples were dissolved in a HF-HNO₃ mixture, evaporated to dryness, redissolved in HCl-HNO₃ then evaporated. Samples were finally redissolved in HNO₃ 2N before Nd chemistry or in 500 μl of HBr 0.8N just before Pb chemistry. Results are reported in Tables S4, S5, and S6.

3.2.1. Nd Isotope Analyses

[12] For core MD99-2254 (Table S4), Sm - Nd concentrations and $^{147}\text{Sm}/^{144}\text{Nd}$ - $^{143}\text{Nd}/^{144}\text{Nd}$ were measured

on a VG Sector 54 mass spectrometer (GEOTOP, Montreal). Sm and Nd concentrations were measured by isotopic dilution using a $^{149}\text{Sm}/^{150}\text{Nd}$ spike. Rare earth elements were separated by using TRU Spec column in HNO₃ environment, then Nd and Sm were successively extracted by using HDEHP column in HCl environment [Richard et al., 1976]. We have followed the analytical procedure outlined by Innocent et al. [1997]. The accuracy and precision was monitored by measurements of AMES Nd standard [Wasserburg et al., 1981], that gave a mean value of $^{143}\text{Nd}/^{144}\text{Nd} = 0.512139 \pm 13$ (2 s.d., $n = 6$). The laboratory mean value for measurements of LaJolla Nd standard [Lugmair and Carlson, 1978; Tanaka et al., 2000] was 0.511849 ± 12 (2 s.d., $n = 21$), i.e., a value close to the mean ratio obtained on 145 measurements (0.511858 ± 7) by Tanaka et al. [2000]. Total blanks were negligible ($\sim 50\text{--}300 \text{ pg}$) in comparison to the quantity of Nd (~ 500 to 1000 ng) or Sm in the sample ($90\text{--}180 \text{ ng}$), i.e., equivalent to 0.005 to 0.05%, and 0.02–0.3% of the total analyzed Nd and Sm from a sample, respectively.

[13] For HU91-045-091 (Table S6) and HU91-045-080 cores (Table S5), the preparation was made in class 100 flow hoods in the clean room at the University of Liege. Sm and Nd concentrations have been analyzed by ICP-MS

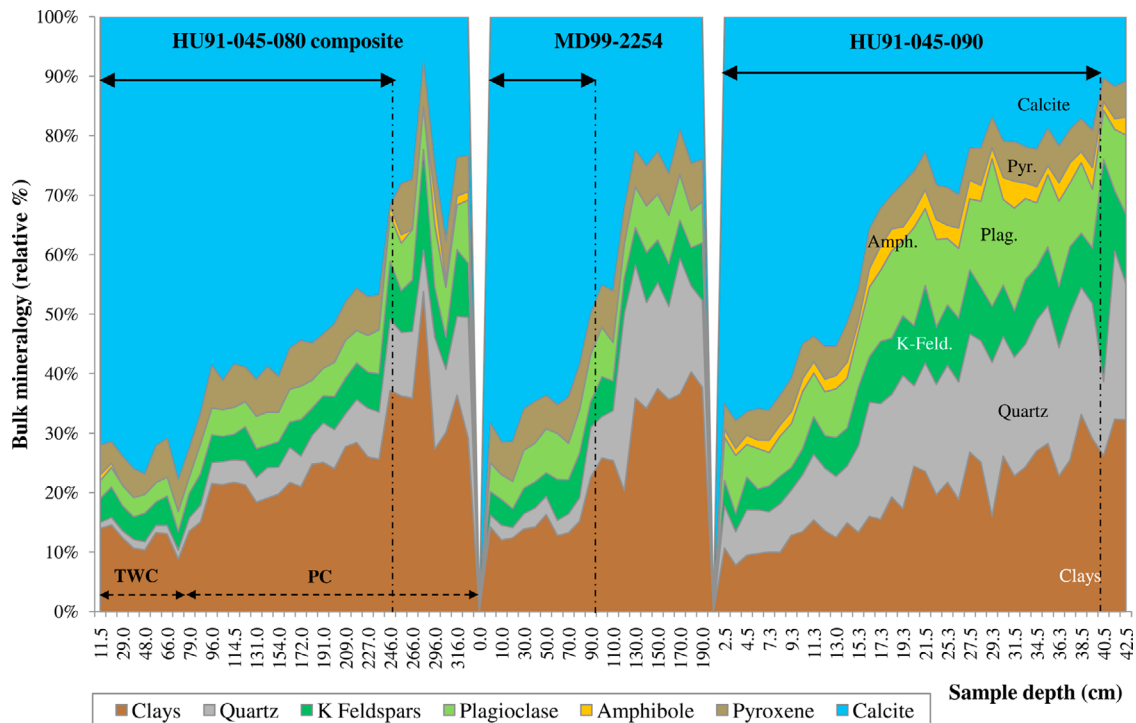


Figure 3. Evolution of the relative contribution of clay minerals, quartz, K-feldspar, plagioclase, amphibole, pyroxene and calcite in the bulk sediment from cores HU91-045-080, MD99-2254 and HU91-045-091. Mineralogical data are deduced from X-ray diffraction measurements on bulk sediment powder (data from Tables S1, S2, and S3). The arrows indicate the Holocene interval.

(MRAC, Tervuren, Belgium). The $^{147}\text{Sm}/^{144}\text{Nd}$ ratios have been calculated from the measured Sm and Nd contents. The $^{143}\text{Nd}/^{144}\text{Nd}$ ratios were measured in static mode using a MC-ICP-MS Nu Plasma instrument in dry mode (ULB, Belgium). The $^{143}\text{Nd}/^{144}\text{Nd}$ ratios have been corrected for mass fractionation assuming a $^{146}\text{Nd}/^{144}\text{Nd}$ ratio of 0.7219 [e.g., Tanaka *et al.*, 2000]. During the analysis session, a solution of 300 ppb of Nd Rennes standard was repeatedly measured between two samples in order to control the instrumental mass bias (applying the correction method of the sample standard bracketing [e.g., Albarède *et al.*, 2004]). The $^{143}\text{Nd}/^{144}\text{Nd}$ values of the Rennes standard solution were stable during the different analysis sessions (0.511944 ± 23 ; 2 s.d. for $n = 128$, 8 days). Those later values are in agreement with the long-term laboratory mean value (0.511946 ± 27 ; 2 s.d. for $n = 516$; r.s.d = 54 ppm), agreeing with the TIMS certified values (0.511963 ± 8 [Chauvel and Blichert-Toft, 2001]).

3.2.2. Pb Isotope Analyses

[14] Pb concentration has been analyzed for HU91-045-080 by ICP-MS (MRAC, Tervuren, Belgium). Lead separation was performed at ULg using successive acid elution on anionic resin (AG1-X8) column (for further details see Weis *et al.* [2006]). The sample solution was loaded on anion exchange columns filled with AG1-X8 resin. After column rinsing with HBr 0.8 N the Pb was eluted by HCl 6N. Collected lead fractions were then evaporated and dried residues were dissolved in 100 μl of concentrated HNO_3 , evaporated and finally dissolved in 1.5 ml of HNO_3 0.05 N. The Pb isotopes were measured on a Nu Plasma MC-ICP-MS instrument (Nu instrument, ULB, Belgium). The

analyses were performed in static mode. Tl was added to each sample and standard to control the instrumental mass bias. Solutions were prepared to obtain a Pb-Tl ratio of 4 or 5, a signal of minimum 100 mV in the axial collector (^{204}Pb) and to reach the Pb and Tl concentrations of the standard (200 ppb of Pb and 50 ppb of Tl). NBS981 international standard was repeatedly measured ($n = 36$) during the 3 analysis sessions. All the measurements were automatically corrected according to the Tl mass fractionation as well as using the sample standard bracketing method with the recommended values of Galer and Abouchami [1998]. The measurements of the NBS981 standard solution performed during our sessions are 36.7152 ± 30 (2 s.d., $n = 31$) for $^{208}\text{Pb}/^{204}\text{Pb}$, 15.4965 ± 12 for $^{207}\text{Pb}/^{204}\text{Pb}$ and 16.9396 ± 14 for $^{206}\text{Pb}/^{204}\text{Pb}$. Such values are in good agreement with the long-term mean values obtained in the laboratory, i.e., 36.7156 ± 89 (2 s.d., $n = 1628$) for $^{208}\text{Pb}/^{204}\text{Pb}$, 15.4970 ± 26 for $^{207}\text{Pb}/^{204}\text{Pb}$ and 16.9405 ± 37 for $^{206}\text{Pb}/^{204}\text{Pb}$. Such ratios are consistent with reference mean values reported by Galer and Abouchami [1998] and Galer [1999]. Duplicates of the entire procedure are reported in Table S5 and show good reproducibility. Total blank (<200 pg) were considered as negligible, representing 0.2 to 0.04% of the Pb quantity in the sample (100–500 ng).

4. Results

4.1. Mineralogy

[15] The principal minerals identified in all the cores are clays, quartz, K-feldspars, plagioclase, pyroxene and calcite. Amphibole is detected only in some samples, with an

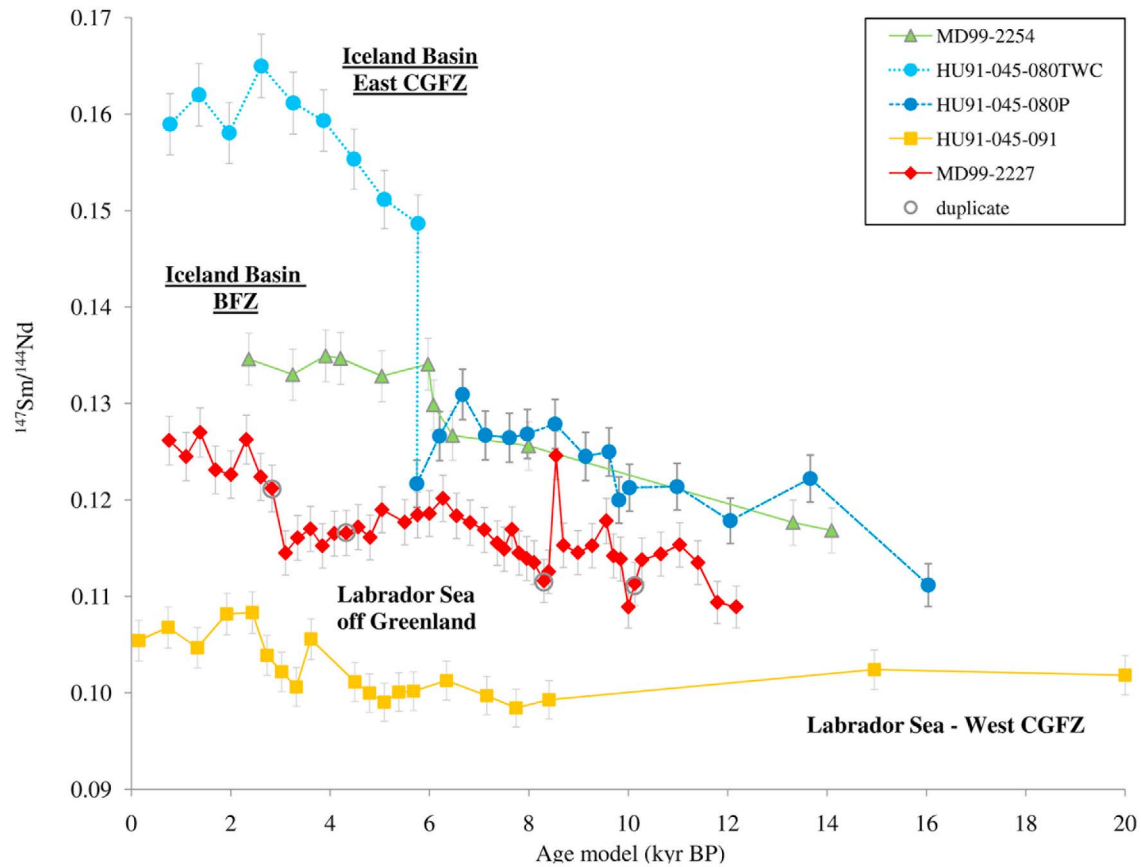


Figure 4a. $^{147}\text{Sm}/^{144}\text{Nd}$ ratios of the clay-size fraction of sediment cores as a function of model ages. Analytical errors are estimated at $\pm 2\%$ of the measured ratio (data for core MD99–2227 from *Fagel et al.* [2004]).

unusual spatial and temporal distribution (Figure 3). Ubiquitous in cores from Labrador Sea (HU91-045-091 and MD99–2227) amphibole is usually absent in the two cores from the Iceland Basin. Totally absent in core MD99–2254, amphibole only occurs as a trace component in the deepest section of core HU91-045-080 (below 250 cm, ≥ 11.8 kyr) as well as in the upper 20 cm (≤ 1.4 kyr).

[16] All other records however are characterized by a marked increase in calcite between the Late Glacial and the Holocene (Figure 3). In the core MD99–2254, the calcite evolves from less than 30% in the Late Glacial samples to 60% in the Holocene samples. The increase occurs in two steps at 17.4 and 8 kyr BP. In the core HU91-045-080, the calcite abundance increases from 25 to 30% during the Late Glacial to 60% during the Holocene, and 70% for the last ~ 6 kyr. In core HU91-045-091, calcite ranges from 10% before glacial/interglacial termination to 20–30% in the first part of Holocene and reaches up to 65% during the last 2 kyr BP. Assuming that calcite is entirely derived from the biological activity, we calculate the relative abundance of the detrital fraction on a calcite-free basis. The composition of the detrital assemblage does not significantly change through the studied interval (with amphibole as an exception) but does vary between cores (Figure 3). Core HU91-045-091 is the most depleted in clays ($< 30\%$ of the detrital

fraction) and relatively enriched in quartz (20% of the detrital fraction).

4.2. Sm, Nd and Pb Geochemistry

[17] The $^{147}\text{Sm}/^{144}\text{Nd}$ ratios display a large range of variation (Figure 4a). The lowest values are recorded in the western Labrador Sea basin in core HU91-045-091 (mean = 0.10); the highest in the eastern Iceland Basin (mean HU91-045-080 = 0.14; mean MD99–2254 = 0.13). The $^{147}\text{Sm}/^{144}\text{Nd}$ ratio reaches a maximum value of 0.16 in core HU91-045-080 (Table S5 and Figure 3). In the eastern basins, the $^{147}\text{Sm}/^{144}\text{Nd}$ ratios increase sharply in the upper core sections. The change occurs ca. 6 kyr in both cores from Iceland Basin but is less pronounced in Bight Fracture Zone (core MD99–2254). In the Labrador Sea, a significant increase was also observed at 3 kyr in core MD99–2227 [*Fagel et al.*, 2004].

[18] The $^{143}\text{Nd}/^{144}\text{Nd}$ isotopic compositions range between low values observed for the Labrador Sea [0.511703 ± 9 (2se) in HU91-045-091] and higher values of the Iceland Basin (mean HU91-045-080 = 0.512334 ± 7 , mean MD99–2254 = 0.512360 ± 13 (Tables S4, S5, and S6)). For the Labrador Sea, the $^{143}\text{Nd}/^{144}\text{Nd}$ values measured in core HU91-045-091 are consistent with the lowest values recorded in core MD99–2227 samples at ca. 8 and 10 kyr [*Fagel et al.*, 2004]. In both cores from the Iceland Basin, a shift in

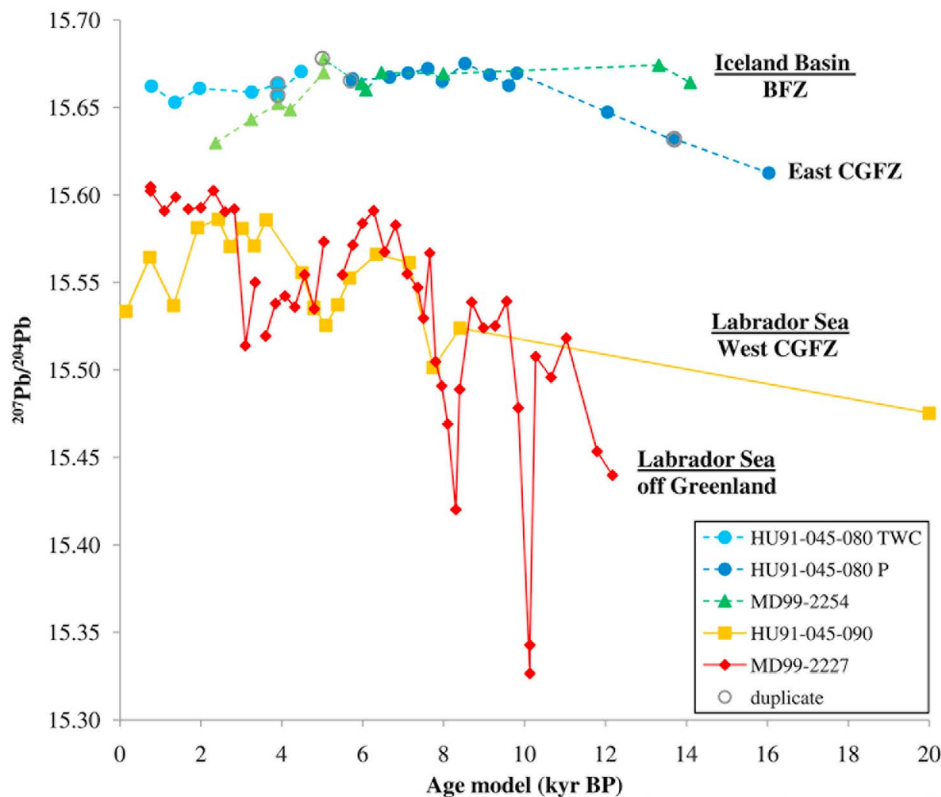


Figure 4b. $^{207}\text{Pb}/^{204}\text{Pb}$ ratios of the clay-size fraction of sediment cores as a function of model ages. Analytical errors are reported (data for core MD99–2227 from *Fagel et al.* [2004]).

$^{143}\text{Nd}/^{144}\text{Nd}$ values is observed at ca. 6 kyr (Figure 5). For instance in core MD99–2254 the $^{143}\text{Nd}/^{144}\text{Nd}$ values increase from 0.5123 to 0.5124 within 500 years.

[19] The $^{206}\text{Pb}/^{204}\text{Pb}$ and $^{207}\text{Pb}/^{204}\text{Pb}$ values ranges from 18.2991 ± 34 (2se) to 19.2384 ± 10 , and from 15.4754 ± 29 to 15.6752 ± 13 , respectively (Tables S4, S5, and S6). Pb isotopic compositions, in particular $^{207}\text{Pb}/^{204}\text{Pb}$, allow a clear distinction between the signatures of the eastern and western Atlantic basins, those ratios being systematically more radiogenic in cores from the Iceland Basin relative to the Labrador Sea (Figure 4b).

5. Discussion

5.1. Identification of Sedimentary Sources

5.1.1. Sm-Nd Mixing Trends

[20] The Nd isotopic data measured on the clay-size fraction of the three studied cores and one previously published MD99–2227 core [*Fagel et al.*, 2004] are reported in a $^{143}\text{Nd}/^{144}\text{Nd}$ versus $^{147}\text{Sm}/^{144}\text{Nd}$ diagram (Figure 5). In such diagram any linear trend defined by core samples may be interpreted as a mixing between at least two end-members. In order to identify the sources we need to compare our data set with the representative isotopic signature of the geological terranes surrounding the northern North Atlantic basins as defined by *Fagel et al.* [2004]. According to the identified regional sources, the composition of the samples from the Iceland Basin may be explained by inputs from young

crustal material (the end-member characterized by the lowest $^{143}\text{Nd}/^{144}\text{Nd}$ and $^{147}\text{Sm}/^{144}\text{Nd}$ ratios) and from volcanic material (the end-member characterized by the highest ratios). Assuming the composition of the two end-members (listed in Table 1), we may estimate the relative contribution of those sources within the mixing (Figure 5).

[21] In core MD99–2254, the volcanic supplies represent less than 10% in the oldest samples and up to 40 to 50% in the youngest; the supplies from young crustal material decreasing from 90% to less than 60%. Likewise the volcanic end-member explains ~10 to 30% of the mixing in the samples older than 6 kyr from core HU91-045-080 and significantly increases in the youngest samples (<6 kyr). The crustal contributions will be further identified using the Pb data (Figure 6).

5.1.2. Pb Mixing Trend

[22] The Pb isotopic data measured on the clay-size fraction of the three studied cores are reported in a $^{207}\text{Pb}/^{204}\text{Pb}$ versus $^{206}\text{Pb}/^{204}\text{Pb}$ diagram (Figure 6). In this diagram the sample distribution allows for the identification of three distinct linear trends, each supporting mixing processes between different two end-member components.

[23] 1. The trend defined by core HU91-045-091 ($r^2 = 0.48$) is consistent with a mixing involving material supplied from the two Labrador Sea margins. The most probable source characterized by a high $^{206}\text{Pb}/^{204}\text{Pb}$ ratio is the Ketilidian Belt (GKB) on the Greenland margin. The low $^{206}\text{Pb}/^{204}\text{Pb}$ candidates are the Grenville Province (GP), with

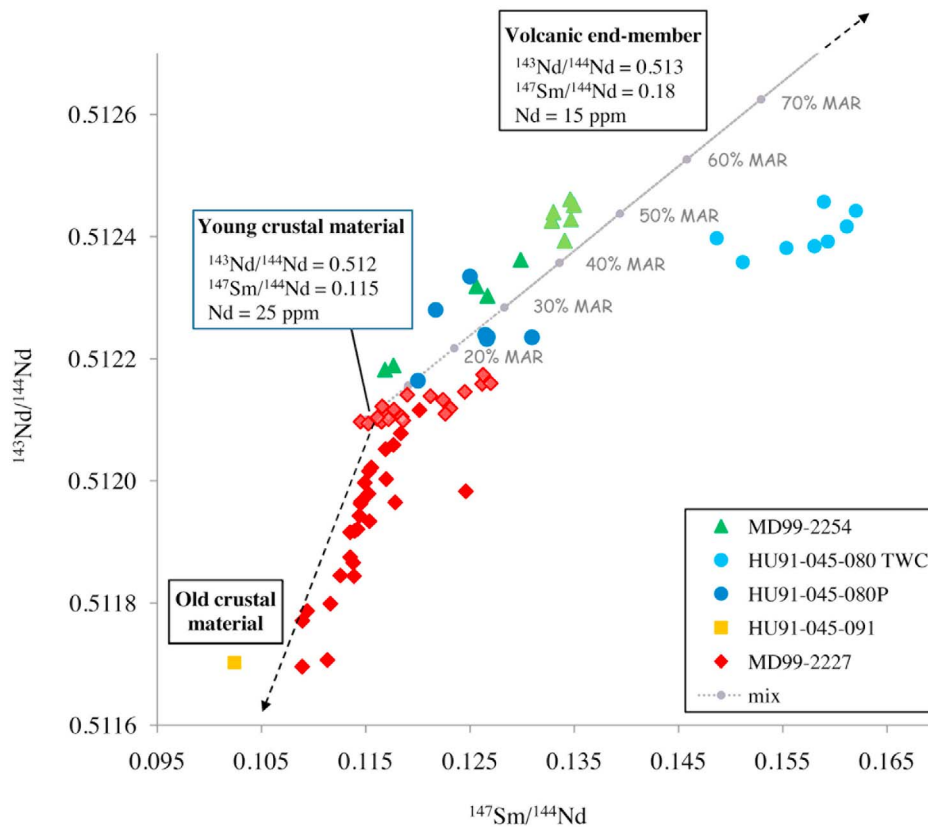


Figure 5. $^{147}\text{Sm}/^{144}\text{Nd}$ versus $^{143}\text{Nd}/^{144}\text{Nd}$ diagram. Data from core MD99–2227 [Fagel *et al.*, 2004] are plotted for comparison. All data are plotted in regard with the potential regional sources (data listed in Table 1). We also report a calculated mixing-line between young crust ($^{143}\text{Nd}/^{144}\text{Nd} = 0.512$, $^{147}\text{Sm}/^{144}\text{Nd} = 0.115$, Nd content = 25 ppm) and volcanic end-member ($^{143}\text{Nd}/^{144}\text{Nd} = 0.513$, Nd content = 15 ppm, $^{147}\text{Sm}/^{144}\text{Nd} = 0.18$). Note the younger samples (<6 kyr) indicated by lighter greys are shifted toward the volcanic end-member. See text for explanation.

eventually some contribution from the Labrador Nain Province (LNP). Such a mixing between material delivered from the southern tip of Greenland (GKB) and the southern (GP) Canadian margin suggests a deep re-circulation gyre within the Labrador.

[24] 2. The trend defined by core MD99–2254 ($r^2 = 0.88$) may be explained by contributions from Variscan and Panafrican crustal material surrounding the eastern Atlantic basins. Taking into account the core location (Figure 1) a mixing between European (EVC) and Scandinavian (SPC) materials is the most probable. Note the youngest (<6 kyr) samples from core HU91-045-080, whose data points are aligned along the same mixing trend ($r^2 = 0.54$).

[25] 3. The third trend is defined by the oldest (>6 kyr) samples from core HU91-045-080 and by all the samples from MD99–2227 (data from Fagel *et al.* [2004]). On one hand the data distribution requires a contribution from old crustal material from Greenland (Archean Craton GAC, Naqssuqtoquidian Belt GNB) or Canadian margins (Labrador Nain Province, LNP) of the Labrador Sea. On the other hand the high $^{206}\text{Pb}/^{204}\text{Pb}$ and $^{207}\text{Pb}/^{204}\text{Pb}$ ratio end-member points to a mixing between Greenland Ketilidian Belt (GKB) and a young crust like the European Variscan Crust (EVC).

5.1.3. Combined Sm, Nd and Pb Mixing Trends

[26] By reporting both Pb and Nd isotopic data (Figure 7a), the number and the identity of the source components are determined in more details; more than two sedimentary supplies are now required to explain the trends described by the data.

[27] The isotope signatures of core MD99–2254 are consistent with a mixing between European young crusts (SPC, EPC) and volcanic material (MAR). Taking into account the $^{207}\text{Pb}/^{206}\text{Pb}$ and $^{143}\text{Nd}/^{144}\text{Nd}$ ratios as well as the Nd and Pb contents of those identified end-members (Table 1) we calculate the corresponding mixing grid (Figure 7a) and we estimate for each sample the relative contribution of those end-members (Figure 7b). We observe an increase of the MAR contribution from 40 to 50% at ~6 kyr and a marked increase of the SPC from 5 to 40% within the last 4 kyr.

[28] For core HU91-045-080 the samples are clustered in two groups. A similar EPC-SPC-MAR mixing grid was used for the youngest (<6 kyr) samples (Figure 7a). The contribution of those latter three end-member in the upper core HU91-080-045 is close to the estimates from core MD99–2254 for the same period, with lower SPC contribution ($\leq 10\%$, Figure 7b). However, the oldest samples (>6 kyr) from core HU91-045-080 lay outside the EPC-SPC-MAR mixing grid (Figure 7a). In addition, as underlined by the Pb

Table 1. Sm, Nd and Pb Isotopic Signature of Geological Terranes Surrounding Northern North Atlantic^a

End-Members	Label	Statistics	¹⁴⁷ Sm/ ¹⁴⁴ Nd	¹⁴³ Nd/ ¹⁴⁴ Nd	²⁰⁶ Pb/ ²⁰⁴ Pb	²⁰⁷ Pb/ ²⁰⁴ Pb	²⁰⁷ Pb/ ²⁰⁶ Pb
Mid-Atlantic volcanism	MAR	mean	0.1877	0.513006	18.641	15.515	0.841
		median	0.1756	0.512997	18.490	15.495	0.839
European Variscan Crust	EVC	mean	0.1144	0.512080	18.840	15.702	0.834
		median	0.1151	0.512074	18.891	15.723	0.831
European Panafrican Crust	EPC	mean	0.1171	0.512045	18.950	15.549	0.821
		median	0.1154	0.512037	18.772	15.529	0.829
Greenland Panafrican crust	GPC	mean	0.115*	0.512*	18.596	15.594	0.839
		median			18.388	15.598	0.848
Scandinavian Panafrican Crust	SPC	mean	0.1052	0.512137	18.451	15.604	0.846
		median	0.1042	0.512160	18.419	15.602	0.847
Scandinavian Sveconorwegian Belt	SSB	mean	0.1257	0.512044	18.925	15.633	0.833
		median	0.1199	0.511980	17.981	15.556	0.864
Greenland Ketilidian belt	GKB	mean	0.1135	0.511697	21.236	15.624	0.757
		median	0.1137	0.511699	20.816	15.653	0.754
Greenland Naqssuqtoqidian Belt	GNB	mean	0.1009	0.511046	16.673	14.920	0.950
		median	0.1007	0.510973	15.227	14.692	0.966
Greenland Archean Craton	GAC	mean	0.0894	0.510671	14.914	14.738	1.003
		median	0.0916	0.510699	14.417	14.417	1.028
Labrador Nain Province	LNP	mean	0.095*		15.684	14.618	0.939
		median			15.986	14.548	0.925
Canadian Grenvillian Province	GP	mean			16.805	15.428	0.919
		median	0.095*		16.867	15.416	0.914
Canadian Superior province	SP	mean	0.1122	0.511200	25.526	16.657	0.711
		median	0.1056	0.511068	22.719	16.226	0.714

^aThe isotopic signatures of the regional sources were defined from literature data: MAR [O'Nions *et al.*, 1977; Carter *et al.*, 1979; Zindler *et al.*, 1979; Cohen *et al.*, 1980; Gariépy *et al.*, 1983] (see full references in the work by *Fagel et al.* [1999]), EVC [Michard *et al.*, 1985; Liew and Hofmann, 1988] (see full references in the work by *Fagel et al.* [1999]), EPC, GPC and SPC [O'Nions *et al.*, 1983; Miller and O'Nions, 1984; Michard *et al.*, 1985; André *et al.*, 1986] (see full references in the work by *Fagel et al.* [1999]), SSB [Andersen *et al.*, 1994; Knudsen *et al.*, 1997], GKB [Patchett and Bridgewater, 1984; Kalsbeek and Taylor, 1985], GNB [Taylor *et al.*, 1980; Kalsbeek *et al.*, 1984, 1988, 1993], GAC [Moorbath *et al.*, 1981; Taylor *et al.*, 1992], LNP [Baadsgaard *et al.*, 1979], GP [Schärer, 1991], SP [Gariépy and Allègre, 1985; Shirey and Hanson, 1986; Barrie and Shirey, 1991; Vervoort *et al.*, 1993; Henry *et al.*, 1998], and WGR [Goldstein and Jacobsen, 1987, 1988; Asmerom and Jacobsen, 1993] (see full references in the work by *Fagel et al.*, 2002]). Mean and median values were calculated in order to take into account the uncertainty of the end-member composition [see *Fagel et al.*, 2002]. The asterisk indicates a default value taking into account the age of the terranes as no Sm-Nd data were available for GPC, LNP and GP. For GPC, we use the same Sm-Nd values as EPC.

data (Figure 6), those oldest samples are characterized by isotopic compositions reflecting additional contribution from old crustal materials from southern Greenland (GKB, GNB). The mixing requires more than 3 sources.

[29] Finally data from the HU91-045-091 core samples lies close to the isotopic field defined by the core MD99-2227 [Fagel *et al.*, 2004]. The composition of that sample reflects contribution from old crustal material, in particular from proximal Greenland margin (GKB, GNB). A better indication of the complex sedimentary mixing is given by plotting the data in a ²⁰⁷Pb/²⁰⁶Pb vs. ¹⁴⁷Sm/¹⁴⁴Nd diagram. Even taking into account a third end-member like the Grenville Province (GP) does not explain all of the measured isotope signatures (Figure 8). An additional contribution from an old craton characterized by lower ¹⁴⁷Sm/¹⁴⁴Nd ratio must be involved in the sedimentary mixing. We observe that the ¹⁴⁷Sm/¹⁴⁴Nd values of the HU91-045-090 samples are shifted toward the representative composition of the West Greenland River (WGR) suspension loads (data from Goldstein and Jacobsen [1987, 1988] and Asmerom and Jacobsen's data given in the work by *Fagel et al.* [2002]), a material that is affected by erosion from Greenland Archean Craton (GAC).

5.2. Evolution of Sedimentary Mixings Over the Holocene

[30] In the southern Labrador Sea the core HU91-045-091 (3870 m) is under the influence of proximal supplies from both Labrador Sea margins (Figure 7a), and is outside of any

influence of deep circulation gyre over the last 20 kyr. We will therefore focus our discussion on the two cores from Iceland Basin. Our geochemical data indicate significant changes in the sedimentary supplies, with a major compositional change at ~6 kyr BP.

[31] Before ~6 kyr BP the Pb signature of core HU91-045-080 involves the contribution of an old craton, regionally outcropping only along the adjacent Labrador Sea margins. Such isotopic observation is in agreement with the regional occurrence of amphibole [e.g., Hemming *et al.*, 1998, 2000] a mineral that is always present in Labrador Sea cores (HU91-045-091 and MD99-2227) but absent in core MD99-2254 from northern Iceland Basin. In core HU91-045-080 amphibole is present in trace amount in the oldest section, from 17.2 to 11.8 kyr then it disappears until 1.4 kyr. The Labrador Sea-affinity is confirmed by both the geochemical and the mineralogical signatures, at least in the deepest section of core HU91-045-080.

[32] At ~6 kyr BP both cores HU91-045-080 and MD99-2254 record a pronounced shift in the ¹⁴⁷Sm/¹⁴⁴Nd ratio (Figure 3). Such changes are due to higher contribution of volcanic-derived material driven by the deep current. In both cores the MAR contribution represents at least 50% of the supplies after 6 kyr (Figure 5). This period coincides in Nordic Seas with the end of the Holocene Climate Optimum [e.g., Rousse *et al.*, 2006]. After a period characterized by minor variation, Rousse *et al.* [2006] emphasized increased oceanic instability linked to climate variations, from 6 kyr in core MD99-2275, North Iceland (water depth 440 m). The

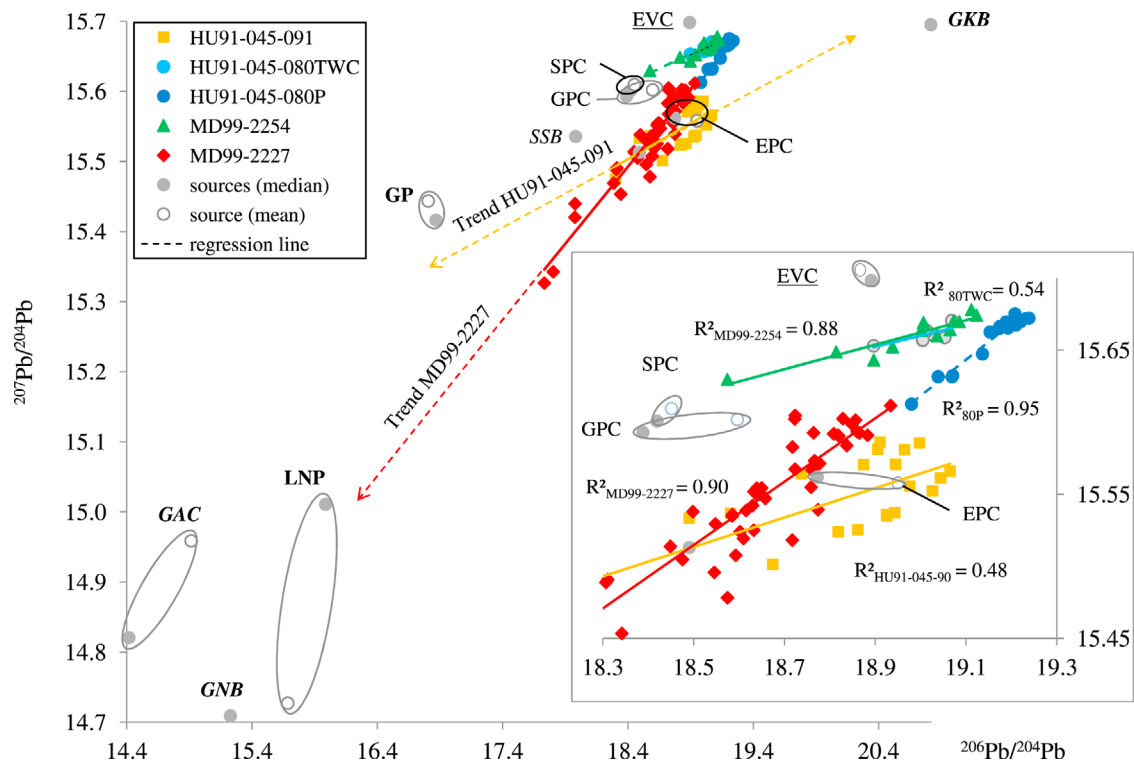


Figure 6. $^{206}\text{Pb}/^{204}\text{Pb}$ versus $^{207}\text{Pb}/^{204}\text{Pb}$ mixing diagram. Data from core MD99–2227 [Fagel *et al.*, 2004] are plotted for comparison. All data are plotted in regard with the potential regional sources. The regional sources are represented by their mean and median values in order to underline the uncertainty of each end-member (data from Fagel *et al.* [2002]). The dashed lines represent the linear regression trend calculated for each core.

variability, deduced from magnetic mineral properties, was mainly associated with the renewed activity of the paleo-Irminger Current in relation with periods of enhanced NADW [Knudsen and Eiriksson, 2002]. Mayewski *et al.* [2004] also evidenced in cores from Iceland Shelf strong fluctuations in grain size parameters after ~ 6 kyr. In Iceland Basin (ODP980, Feni drift, 2179 m), Oppo *et al.* [2003] reported a long-term reduction in NADW contribution beginning at 6.5 kyr. Those long-term records all demonstrated that a major change in the regional oceanography took place at ~ 6 kyr, most likely in relation with, as suggested by Rouse *et al.* [2006], the neoglacial cooling of the surface waters observed in the Denmark Strait [Bond *et al.*, 1997].

[33] After this major change the sedimentary mixing does not change significantly in core HU91-045-080, except for a slight contribution from SCP (5%) during the last 4 kyr BP. However, in core MD99–2254, we note a progressive dilution of EPC by increasing supplies from Northern Europe (SPC). The SCP contribution first represents 5 to 10% of the mixture ca. 6 kyr, it is $>20\%$ at 4.2 kyr and reaches finally 40% at 2.4 kyr BP (Figure 7b).

5.3. Paleoceanographic Implications on North Atlantic Deep Circulation

[34] Our mineralogical and geochemical proxies indicate changes in sedimentary mixings driven by the deep current over the Holocene. Such changes indirectly support significant modifications in the relative contribution of the

different water masses involved in North Atlantic Deep Water. The timing of the main current reorganizations (8, 6, 3 kyr) discussed is consistent with the general Holocene climate pattern in the North Atlantic [Andersen *et al.*, 2004b], with the Holocene Climate Optimum (9.5–6.5 kyr BP), the Holocene Transition period (6.5–3 kyr BP) and the cool late Holocene period (0–3 kyr BP).

5.3.1. The Late Holocene Optimum Period

5.3.1.1. Renewed Iceland-Scotium Overflow Water

[35] The influence of MAR supplies in both cores from the Iceland Basin supports, at least for the last 10 kyr (14 kyr in MD99–2254), the establishment of a southward current following the Mid-Atlantic Ridge, i.e., the southern branch of the ISOW (Figure 1). The Late Holocene Optimum period is characterized by increasing MAR supplies (Figure 7b), driven by ISOW. The hiatus observed between 8 and 12 kyr BP in the sedimentary record of core MD99–2254 coincides with a peak in sedimentation rates in many cores from upper and lower continental slopes in the Iceland Basin (see references given in the work by Kissel *et al.* [2009]). The high sedimentation rate is attributed to remobilization of glacial sediments by the renewed ISOW at the end of the deglaciation [Kissel *et al.*, 2009].

5.3.1.2. E-W Deep Water Exchanges Through CGFZ

[36] Before 6 kyr, our mineralogical and isotopic results indicate a connection between the western and eastern Atlantic basins through the Charlie Gibbs Fracture Zone (CGFZ). Indeed the Labrador-derived supplies must pass through the CGFZ to reach the coring site HU91-045-080.

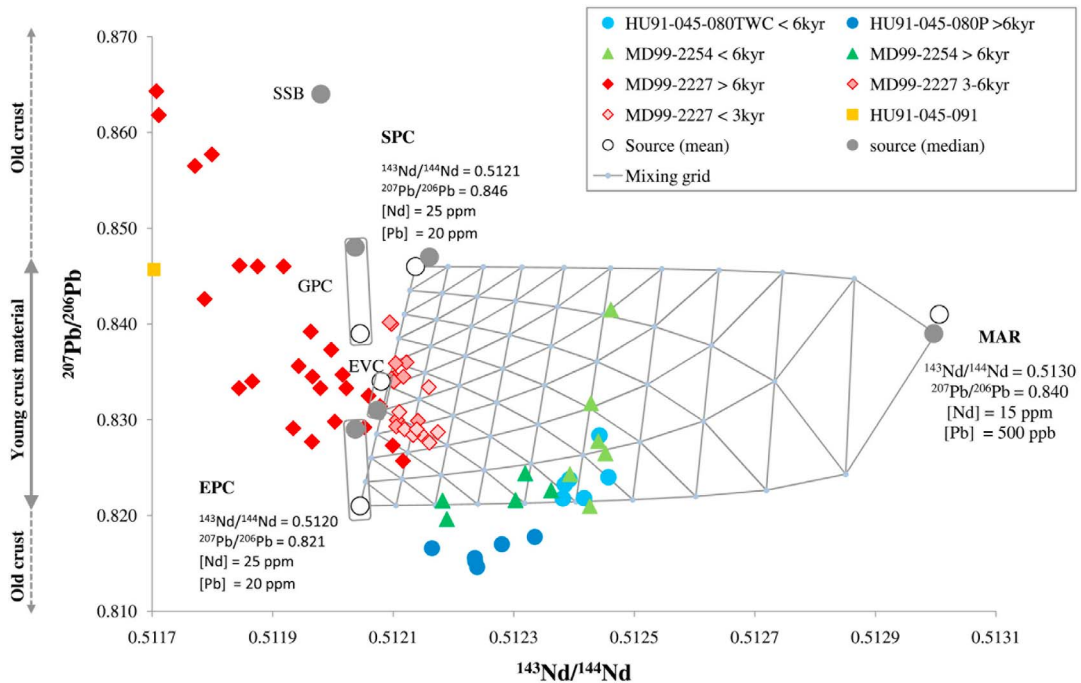


Figure 7a. $^{207}\text{Pb}/^{206}\text{Pb}$ versus $^{143}\text{Nd}/^{144}\text{Nd}$. The mixing grid has been calculated taking into account the $^{207}\text{Pb}/^{206}\text{Pb}$ and the Pb and Nd contents of the retained end-members, i.e., crustal material from Europe (EPC) and Scandinavia (SPC) and volcanic-derived material (MAR). We use this mixing grid EPC-SPC-MAR to estimate the relative contribution from the different regional sources over time, in core MD99–2254 and in core HU91-045-080 but only over the last 6 kyr BP. The results are reported as cumulated histogram in Figure 7b.

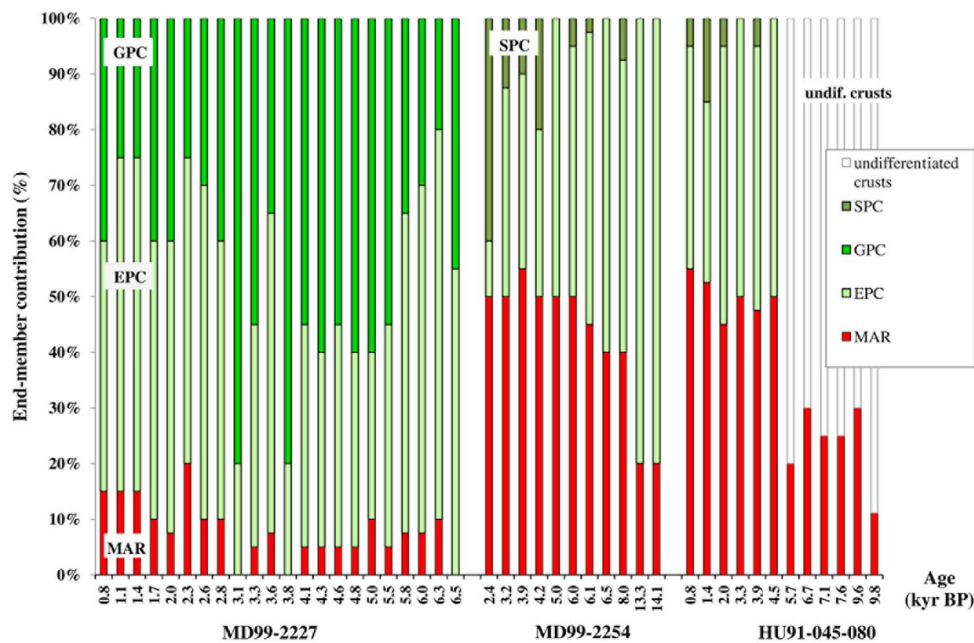


Figure 7b. Temporal changes of estimated contributions are reported as cumulated histograms. The contributions for the core MD99–2254 and upper part of core HU91-045-080 have been estimated using the mixing grid EPC-SPC-MAR reported in Figure 7a. As more than 3 end-members are requested to explain the data for the lower part of core HU91-045-080 (samples \geq 6 kyr) we have only estimated the contribution of MAR using the mixing line reported on Figure 5. Data for core MD99–2227 are from *Fagel et al.* [2004]. See text for explanation.

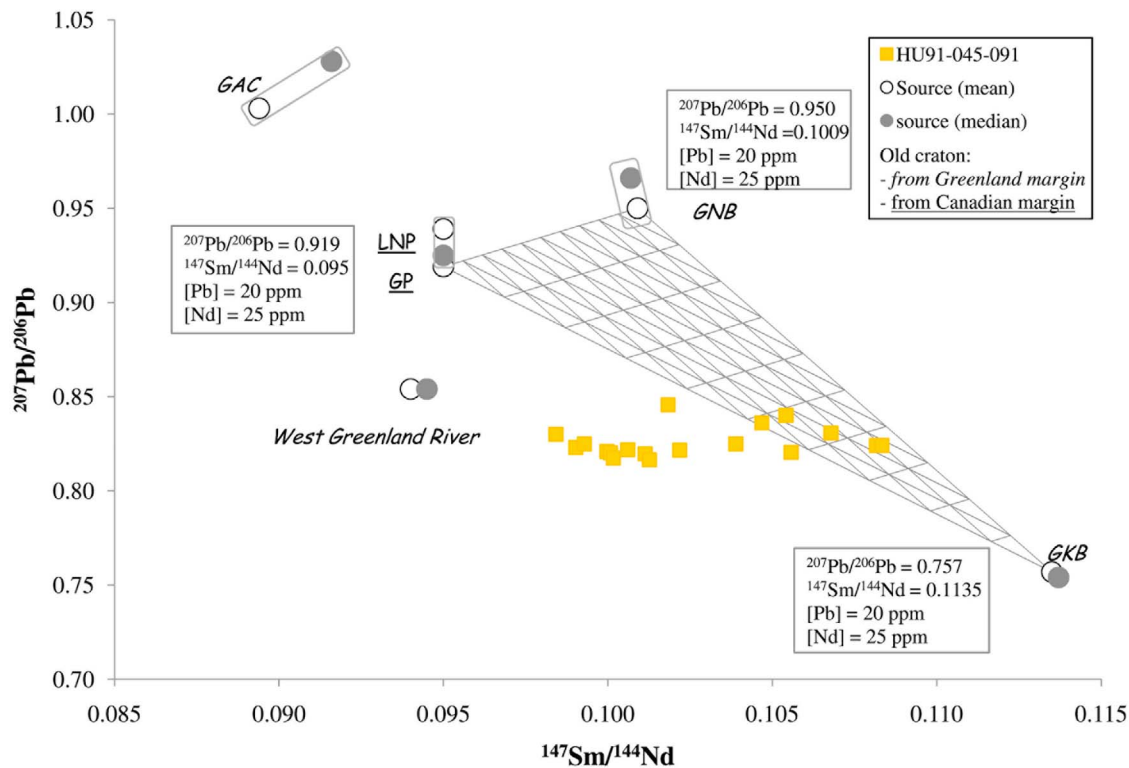


Figure 8. $^{207}\text{Pb}/^{206}\text{Pb}$ versus $^{147}\text{Sm}/^{144}\text{Nd}$. Data from core HU91-045-090 are reported in regard with the representative values of the crustal material outcropping along the Greenland and Canadian margins of Labrador Sea. Each end-member is characterized by mean and median values (values listed in Table 1; for statistics and data see *Fagel et al.* [2002]). The grid is calculated according to a 10% increment of the mixture composition. It takes into account the $^{207}\text{Pb}/^{206}\text{Pb}$ and the Pb, Sm and Nd contents of the 3 end-members GP, GNB and GKB. See text for explanation.

East–west water’s exchange is not surprising as CGFZ is, at present, characterized by a complex ocean circulation system [e.g., *Lucotte and Hillaire-Marcel*, 1994]. After 6 kyr our Pb data no longer support exchange through the CGFZ, at least until the last 1.4 kyr. Trace of amphibole is evidenced until ~ 12 kyr, interrupted between at least 6 and 1.4 kyr BP. This trace in the upper section may suggest some, but limited, East–west water exchange through the CGFZ over the last 1.4 kyr as the geochemical composition does not change significantly.

5.3.2. The Holocene Transition Period (6.5–3 kyr BP): Reinforcement of ISOW

[37] Sedimentological and geochemical changes are not synchronous in eastern and western basins. They occur earlier in eastern basins than in Labrador Sea. Indeed cores HU91-045-080 and MD99–2254 are characterized by a pronounced shift in the geochemical signatures, with a sharp increase of $^{147}\text{Sm}/^{144}\text{Nd}$ ratio at 6 kyr. A similar later change (3 kyr) was previously observed in core MD99–2227 [*Fagel et al.*, 2004]. Such changes are due to higher contributions of volcanic-derived material driven by the deep current. In cores HU91-045-080 and MD99–2254 these changes may be related to the circulation of the southwards branch of the NEADW that follows the Mid-Atlantic Ridge, i.e., NEADW 2 according to *Lucotte and Hillaire-Marcel* [1994] or ISOW according to *Kissel et al.* [2009]. In the Iceland Basin the present source of deep water originates from Fram or

Denmark straits [*Aagaard and Carmack*, 1989]. Until 7–6 kyr the Arctic outflow was considered to be larger from the Canadian channels than from the Denmark Strait [*Williams et al.*, 1995]. The inception of eastern branches of NADW, DSOW and NEADW, may therefore be related to the final melting of the remaining Canadian ice sheets. The shallowing of the Canadian channels then limits the outflow into Labrador Sea after 7.4 kyr [*Solignac et al.*, 2004]. At the same time the inception of eastern deep currents may break down any western supplies through the CGFZ as seen in core HU91-045-080.

[38] Recently *Kissel et al.* [2009] reported long-term variations in the ISOW flow over the Holocene. They interpreted the decreasing trend of the mineral magnetic content in 6 cores from Iceland Basin as a decrease of the ISOW bottom current strength over the Holocene. However, they noticed that their hypothesis was inconsistent with the short-term variations derived from deep-sea proxies [*Bianchi and McCave*, 1999; *Oppo et al.*, 2003; *Hall et al.*, 2004; *Praetorius et al.*, 2008]. Our geochemical observations in both cores from Iceland Basin are rather in favor of a continuous depletion of the detrital supply, an alternative hypothesis that *Kissel et al.* [2009] did not rule out.

5.3.3. The Cool Late Holocene Period (0–3 kyr BP): Reinforcement of Norwegian Sea Overflow Water

[39] Our Pb data suggest a late change in the sedimentary mixings in the Iceland Basin. In core MD99–2254 a

significant shift of the $^{207}\text{Pb}/^{206}\text{Pb}$ ratios out off the EPC field (Figure 7a) is obvious for the 2 youngest samples (≤ 3 kyr). Beside the EPC contribution the mixing requires the contribution from another crustal material, the EVC or the SPC. According to the core location we suggest a recent activation of the northern branch of the East Atlantic deep current like AIW or Norwegian Sea Overflow Water (NSOW), a current containing an isotopic signature derived from the erosion of the Scandinavian margin (SPC). Such recent changes may be related to a change in surface circulation, likely related to a strengthening of the NAW.

6. Conclusion

[40] On the basis of combined geochemical and mineralogical studies, we have identified the main sedimentary supplies and their fluctuating contributions over the Holocene in eastern and western North Atlantic basins.

[41] The origin of the sedimentary supplies driven by the deep current remain constant in cores HU91-045-090 (from Canadian and Greenland margins) and MD99-2254 (from western European margin and Mid-Atlantic Ridge volcanic province). In contrast, a sharp change in the involved sources is observed in core HU90-045-080 at ~ 6 kyr. Before 6 kyr distal supplies from Greenland margin were driven into the Iceland Basin, supporting a deep connection between the Labrador Sea and the Iceland Basin through CGFZ.

[42] The main paleoceanographical interpretations from our elemental and isotopic Nd and Pb data obtained on cores from the Iceland Basin and the Labrador Sea are: a renewal of the southwards branch of the ISOW during the Late Holocene Optimum; its reinforcement at the beginning of the Holocene Transition Period (~ 6 kyr BP) and a late reinforcement of the NSOW during the cool Late Holocene period (last 3 kyr). The timing of the main deep current reorganization is consistent with the general Holocene climate patterns previously defined in the North Atlantic.

[43] **Acknowledgments.** We acknowledge all the persons who have contributed to this study for sampling access, technical assistance or scientific discussion, mainly C. Hillaire-Marcel, Helene Isnard and R. Stevenson at Geotop (Uqam, Montreal); D. Weis, C. Maerschalk and J. de Jong at DSTE (ULB, Brussels) and C. Innocent at BRGM (France). R. Brasseur, L. Colin, D. Ménager have performed part of the reported mineralogical and/or geochemical analyses within the framework of their master thesis at AGEs, Department of Geology, ULg. The authors thank the two anonymous reviewers for their attentive reading of the manuscript and their constructive comments. This work was mainly funded by FNRS (grant 2.4.530.05.F).

References

- Aagaard, K., and E. C. Carmack (1989), The role of sea ice and other fresh water in the Arctic circulation, *J. Geophys. Res.*, *94*, 14,485–14,498, doi:10.1029/JC094iC10p14485.
- Albarède, F., P. Têlouk, J. Blichert-Toft, M. Boyet, A. Agranier, and B. Nelson (2004), Precise and accurate isotopic measurements using multiple-collector ICPMS, *Geochim. Cosmochim. Acta*, *68*, 2725–2744, doi:10.1016/j.gca.2003.11.024.
- Andersen, C., N. Koç, A. E. Jennings, and J. T. Andrews (2004a), Nonuniform response of the major surface currents in the Nordic Seas to insolation forcing: Implications for the Holocene climate variability, *Paleoceanography*, *19*, PA2003, doi:10.1029/2002PA000873.
- Andersen, C., N. Koç, and M. Moros (2004b), A highly unstable Holocene climate in the subpolar North Atlantic: Evidence from diatoms, *Quat. Sci. Rev.*, *23*(20–22), 2155–2166, doi:10.1016/j.quascirev.2004.08.004.
- Andersen, T., P. Hagelia, and M. J. Whitehouse (1994), Precambrian multi-stage crustal evolution in the Bamble sector of Norway: Pb isotopic evidence from a Sveconorwegian deep-seated granitic intrusion, *Chem. Geol.*, *116*, 327–343, doi:10.1016/0009-2541(94)90023-X.
- André, L., S. Deutsch, and J. Hertogen (1986), Trace element and Nd isotopes in shales as indexes of provenance and crustal growth: The early Paleozoic from the Brabant massif (Belgium), *Chem. Geol.*, *57*, 101–115, doi:10.1016/0009-2541(86)90096-3.
- Asmerom, Y., and S. B. Jacobsen (1993), The Pb isotopic evolution of the Earth: Inferences from river water suspended loads, *Earth Planet. Sci. Lett.*, *115*, 245–256, doi:10.1016/0012-821X(93)90225-X.
- Baadsgaard, H., K. D. Collerson, and D. Bridgewater (1979), The Archean gneiss complex of northern Labrador. 1. Preliminary U-Th-Pb geochronology, *Can. J. Earth Sci.*, *16*, 951–961, doi:10.1139/e79-081.
- Barrie, C. T., and S. B. Shirey (1991), Nd- and Sr-isotope systematics from the Kamiskotia-Montcalm area: Implications for the formation of late Archean crust in the western Abitibi Subprovince, Canada, *Can. J. Earth Sci.*, *28*(1), 58–76, doi:10.1139/e91-006.
- Bayon, G., C. R. German, R. W. Nesbitt, P. Bertrand, and R. R. Schneider (2003), Increased input of circumpolar deep water-borne detritus to the glacial SE Atlantic Ocean, *Geochem. Geophys. Geosyst.*, *4*(3), 1025, doi:10.1029/2002GC000371.
- Berner, K. S., N. Koç, D. Divine, F. Godtliessen, and M. Moros (2008), A decadal-scale Holocene sea surface temperature record from the subpolar North Atlantic constructed using diatoms and statistics and its relation to other climate parameters, *Paleoceanography*, *23*, PA2210, doi:10.1029/2006PA001339.
- Bianchi, G. G., and I. N. McCave (1999), Holocene periodicity in North Atlantic climate and deep-ocean flow south of Iceland, *Nature*, *397*, 515–517, doi:10.1038/17362.
- Bond, G., W. Showers, M. Cheseby, R. Lotti, P. Almasi, P. de Menocal, P. Priore, H. Cullen, I. Hajdas, and G. Bonani (1997), A pervasive millennial-scale cycle in North Atlantic Holocene and glacial climates, *Science*, *278*, 1257–1266, doi:10.1126/science.278.5341.1257.
- Boski, T., J. Pessoa, P. Pedro, J. Thorez, J. M. A. Dias, and I. R. Hall (1998), Factors governing abundance of hydrolysable amino acids in the sediments from the NW European Continental margin (47–50°N), *Prog. Oceanogr.*, *42*, 145–164, doi:10.1016/S0079-6611(98)00032-9.
- Bridgewater, D., M. Marker, and F. Mengel (1991), The eastern extension of the early Proterozoic orogenic zone across the Atlantic, in *East. Can. Shield Onshore-Offshore Transect Meet. Rep. 34*, 100–107, École Polytech., Montreal, Que., Canada.
- Campbell, L. M., D. Bridgewater, and G. L. Farmer (1996), A comparison of Proterozoic crustal formation along the Torngat-Naqssaqtoqidian-Lapland collision belts: Preliminary constraints from Nd and Pb isotopic studies in Northern Labrador, in *East. Can. Shield Onshore-Offshore Transect Meet. Rep. 45*, pp. 22–36, Ottawa, Ont., Canada.
- Carter, S. R., N. M. Evensen, P. J. Hamilton, and R. K. O'Nions (1979), Basalt magma sources during the opening of the North Atlantic, *Nature*, *281*, 28–30, doi:10.1038/281028a0.
- Chauvel, C., and J. Blichert-Toft (2001), A hafnium isotope and trace element perspective on melting of the depleted mantle, *Earth Planet. Sci. Lett.*, *190*, 137–151, doi:10.1016/S0012-821X(01)00379-X.
- Cohen, R. S., N. M. Evensen, P. J. Hamilton, and R. K. O'Nions (1980), U-Pb, Sm-Nd and Rb-Sr systematics of mid-ocean ridge basalt glasses, *Nature*, *283*, 149–153, doi:10.1038/283149a0.
- Colin, C., N. Frank, K. Copard, and E. Douville (2010), Neodymium isotopic composition of deep-sea corals from the NE Atlantic: Implications for past hydrological changes during the Holocene, *Quat. Sci. Rev.*, *29*(19–20), 2509–2517, doi:10.1016/j.quascirev.2010.05.012.
- Cook, H. E., P. D. Johnson, J. C. Matti, and I. Zemmels (1975), Methods of sample preparation and X-ray diffraction analysis in X-ray mineralogy laboratory, in *Deep Sea Drilling Project Initial Reports*, vol. 28, edited by A. G. Kaneps et al., pp. 997–1007, Tex. A&M Univ., College Station.
- Copard, K., C. Colin, E. Douville, A. Freiwald, G. Gudmundsson, B. De, B. Mol, and N. Frank (2010), Nd isotopes in deep-sea corals in the North-eastern Atlantic, *Quat. Sci. Rev.*, *29*(19–20), 2499–2508, doi:10.1016/j.quascirev.2010.05.025.
- Dickson, R. R., and J. Brown (1994), The production of North Atlantic Deep water: Sources, rates, and pathways, *J. Geophys. Res.*, *99*, 12,319–12,341, doi:10.1029/94JC00530.
- Fagel, N., and C. Hillaire-Marcel (2006), Glacial/interglacial instabilities of the Western Boundary Under Current during the last 360 kyr from Sm/Nd signatures of sedimentary clay fractions at ODP-Site 646 (Labrador Sea), *Mar. Geol.*, *232*, 87–99, doi:10.1016/j.margeo.2006.08.006.
- Fagel, N., C. Innocent, R. K. Stevenson, and C. Hillaire-Marcel (1999), Deep circulation changes in the Labrador Sea since the Last Glacial Maximum: New constraints from Sm-Nd data on sediments, *Paleoceanography*, *14*, 777–788, doi:10.1029/1999PA000041.
- Fagel, N., C. Innocent, C. Gariépy, and C. Hillaire-Marcel (2002), Sources of Labrador Sea sediments since the Last Glacial Maximum inferred from

- Nd-Pb isotopes, *Geochim. Cosmochim. Acta*, 66, 2569–2581, doi:10.1016/S0016-7037(02)00866-9.
- Fagel, N., C. Hillaire-Marcel, M. Humblet, R. Brasseur, D. Weis, and R. Stevenson (2004), Nd and Pb isotope signatures of the clay-size fraction of Labrador Sea sediments during the Holocene: Implications for the inception of the modern deep circulation pattern, *Paleoceanography*, 19, PA3002, doi:10.1029/2003PA000993.
- Frank, M. (2002), Radiogenic isotopes: Tracers of past ocean circulation and erosional input, *Rev. Geophys.*, 40(1), 1001, doi:10.1029/2000RG000094.
- Galer, S. J. G. (1999), Optimal double and triple spiking for high precision lead isotopic measurement, *Chem. Geol.*, 157, 255–274, doi:10.1016/S0009-2541(98)00203-4.
- Galer, S. J. G., and W. Aouchami (1998), Practical application of lead triple spiking for correction of instrumental mass discrimination, 8th Goldschmidt Conf., *Mineral. Mag.*, 62A, 491–492, doi:10.1180/minmag.1998.62A.1.260.
- Gariépy, C., and C. J. Allègre (1985), The lead isotope geochemistry and geochronology of late-kinematic intrusives from the Abitibi greenstone belt, and implications for the late Archean crustal evolution, *Earth Planet. Sci. Lett.*, 49, 2371–2383.
- Gariépy, C., J. Ludden, and C. Brooks (1983), Isotopic and trace element constraints on the genesis of the Faeroe lava pile, *Earth Planet. Sci. Lett.*, 63, 257–272, doi:10.1016/0012-821X(83)90041-9.
- Giraudeau, J., A. E. Jennings, and J. T. Andrews (2004), Timing and mechanisms of surface and intermediate water circulation changes in the Nordic Seas over the last 10,000 cal years: A view from the North Iceland shelf, *Quat. Sci. Rev.*, 23(20–22), 2127–2139, doi:10.1016/j.quascirev.2004.08.011.
- Giraudeau, J., M. Grelaud, S. Solignac, J. T. Andrews, M. Moros, and E. Jansen (2010), Millennial-scale variability in Atlantic water advection to the Nordic Seas derived from Holocene coccolith concentration records, *Quat. Sci. Rev.*, 29(9–10), 1276–1287, doi:10.1016/j.quascirev.2010.02.014.
- Goldstein, S. J., and S. B. Jacobsen (1987), The Nd and Sr isotopic systematics of river water dissolved material: Implications for the sources of Nd and Sr in seawater, *Chem. Geol.*, 66, 245–272.
- Goldstein, S. J., and S. B. Jacobsen (1988), Nd and Sr isotopic systematics of river water suspended material: Implications for crustal evolution, *Earth Planet. Sci. Lett.*, 87, 249–265, doi:10.1016/0012-821X(88)90013-1.
- Gutjahr, M., M. Frank, C. H. Stirling, V. Klemm, T. van de Fliedert, and A. N. Halliday (2007), Reliable extraction of a deepwater trace metal isotope signal from Fe-Mn oxyhydroxide coatings of marine sediments, *Chem. Geol.*, 242(3–4), 351–370, doi:10.1016/j.chemgeo.2007.03.021.
- Gutjahr, M., B. A. A. Hoogakker, M. Frank, and I. N. McCave (2010), Changes in North Atlantic deep water strength and bottom water masses during Marine Isotope Stage 3 (45 to 35 ka BP), *Quat. Sci. Rev.*, 29(19–20), 2451–2461, doi:10.1016/j.quascirev.2010.02.024.
- Hall, I. R., G. G. Bianchi, and J. R. Evans (2004), Centennial to millennial scale Holocene climate-deep water linkage in the North Atlantic, *Quat. Sci. Rev.*, 23(14–15), 1529–1536, doi:10.1016/j.quascirev.2004.04.004.
- Hemming, S. R., W. S. Broecker, W. D. Sharp, G. C. Bond, R. H. Gwiazda, J. F. McManus, M. Klas, and I. Hadjis (1998), Provenance of Heinrich layers in core V28–82, northeastern Atlantic: $^{40}\text{Ar}/^{39}\text{Ar}$ ages of ice-rafted homblende, Pb isotopes in feldspar grains, and Nd-Sr-Pb isotopes in the fine sediment fraction, *Earth Planet. Sci. Lett.*, 164, 317–333, doi:10.1016/S0012-821X(98)00224-6.
- Hemming, S. R., R. H. Gwiazda, J. T. Andrews, W. S. Broecker, A. E. Jennings, and R. Onstott (2000), $^{40}\text{Ar}/^{39}\text{Ar}$ and Pb-Pb study of individual homblende and feldspar grains from southeastern Baffin Island glacial sediments: Implications for the provenance of the Heinrich layers, *Can. J. Earth Sci.*, 37, 879–890, doi:10.1139/e00-009.
- Henry, P., R. K. Stevenson, and C. Gariépy (1998), Late Archean mantle composition and crustal growth in Western Superior Province of Canada: Neodymium and lead isotopic evidence from the Wawa, Quetico, and Wabigoon subprovinces, *Geochim. Cosmochim. Acta*, 62(1), 143–157, doi:10.1016/S0016-7037(97)00324-4.
- Hillaire-Marcel, C., A. de Vernal, S. Vallières, et Équipes Scientifiques (1991), *CSS Hudson 91–045, the Labrador Sea, the Irminger and Iceland Basins*, cruise report, Comm. Géologique du Canada, Vancouver, B. C.
- Innocent, C., N. Fagel, R. K. Stevenson, and C. Hillaire-Marcel (1997), Sm-Nd signature of modern and late Quaternary sediments from the northwest North Atlantic: Implications for deep current changes since the Last Glacial Maximum, *Earth Planet. Sci. Lett.*, 146, 607–625, doi:10.1016/S0012-821X(96)00251-8.
- Jeandel, C., J. K. Bishop, and A. Zindler (1995), Exchange of neodymium and its isotope between seawater and small and large particles in the Sargasso Sea, *Geochim. Cosmochim. Acta*, 59, 535–547, doi:10.1016/0016-7037(94)00367-U.
- Jones, C. E., A. N. Halliday, D. K. Rea, and R. M. Owen (1994), Neodymium isotopic variations in the North Pacific modern silicate sediment and their significance of detrital REE contributions to seawater, *Earth Planet. Sci. Lett.*, 127, 55–66, doi:10.1016/0012-821X(94)90197-X.
- Kalsbeek, F., and P. N. Taylor (1985), Isotopic and chemical variation in granites across a Proterozoic continental margin—the Ketilidian mobile belt of South Greenland, *Earth Planet. Sci. Lett.*, 73, 65–80, doi:10.1016/0012-821X(85)90035-4.
- Kalsbeek, F., P. N. Taylor, and N. Henriksen (1984), Age of rocks, structure, and metamorphism in the Nagssugtoqidian mobile belt, west Greenland-field and Pb-isotope evidence, *Can. J. Earth Sci.*, 21, 1126–1131, doi:10.1139/e84-117.
- Kalsbeek, F., P. N. Taylor, and R. T. Pidgeon (1988), Unreworked Archean basement and Proterozoic supracrustal rocks from northeastern Dikso Bugt, west Greenland: Implications for the nature of Proterozoic mobile belts in Greenland, *Can. J. Earth Sci.*, 25, 773–782, doi:10.1139/e88-072.
- Kalsbeek, F., H. Austrheim, D. Bridgewater, B. T. Hansen, S. Pedersen, and P. N. Taylor (1993), Geochronology of Archean and Proterozoic events in the Ammassalik area, south-east Greenland, and comparisons with the Lewisian of Scotland and the Nagssugtoqidian of west Greenland, *Precambrian Res.*, 62, 239–270, doi:10.1016/0301-9268(93)90024-V.
- Kissel, C., C. Laj, T. Mulder, C. Wandres, and M. Cremer (2009), The magnetic fraction: A tracer of deep water circulation in the North Atlantic, *Earth Planet. Sci. Lett.*, 288, 444–454, doi:10.1016/j.epsl.2009.10.005.
- Knudsen, K.-L., and J. Eiriksson (2002), Application of tephrochronology to the timing and correlation of palaeoceanographic events recorded in Holocene and late Glacial shelf sediments off north Iceland, *Mar. Geol.*, 191, 165–188, doi:10.1016/S0025-3227(02)00530-3.
- Knudsen, T. L., T. Andersen, C. Maijer, and R. H. Verschure (1997), Trace-element characteristics and Pb isotopic evolution of metasediments and associated Proterozoic rocks from the amphibolite- to granulite- Bamble sector, southern Norway, *Chem. Geol.*, 143, 145–169, doi:10.1016/S0009-2541(97)00111-3.
- Lacan, F., and C. Jeandel (2005), Neodymium isotopes as a new tool for quantifying exchange fluxes at the continent-ocean interface, *Earth Planet. Sci. Lett.*, 232, 245–257, doi:10.1016/j.epsl.2005.01.004.
- Liew, T. C., and A. W. Hofmann (1988), Precambrian crustal components, plutonic associations, plate environment of the Hercynian Fold Belt of central Europe: Indications from a Nd and Sr isotopic study, *Contrib. Mineral. Petrol.*, 98, 129–138, doi:10.1007/BF00402106.
- Lucotte, M., and C. Hillaire-Marcel (1994), Identification des masses d'eau dans les mers du Labrador et d'Irminger, *Can. J. Earth Sci.*, 31, 5–13, doi:10.1139/e94-002.
- Lugmair, G. W., and R. W. Carlson (1978), The Sm-Nd history of KREEP, *Proc. Lunar Planet. Sci. Conf.*, 9th, 689–704.
- Martin, E. E., and B. A. Haley (2000), Fossil fish teeth as proxies for sea water Sr and Nd isotopes, *Geochim. Cosmochim. Acta*, 64(5), 835–847, doi:10.1016/S0016-7037(99)00376-2.
- Mayewski, P. A., et al. (2004), Holocene climate variability, *Quat. Res.*, 62(3), 243–255, doi:10.1016/j.yqres.2004.07.001.
- McCartney, M. S. (1992), Recirculating components to the deep boundary current of the northern North Atlantic, *Prog. Oceanogr.*, 29, 283–383, doi:10.1016/0079-6611(92)90006-L.
- McCulloch, M. T., and G. J. Wasserburg (1978), Sm-Nd and Rb-Sr chronology of continental crust formation, *Science*, 200, 1003–1011, doi:10.1126/science.200.4345.1003.
- Michard, A., P. Gurriet, M. Soudaut, and F. Albarède (1985), Nd isotopes in French Phanerozoic shales: External vs. internal aspects of crustal evolution, *Geochim. Cosmochim. Acta*, 49, 601–610, doi:10.1016/0016-7037(85)90051-1.
- Miller, R. G., and R. K. O'Nions (1984), The provenance and residence ages of British sediments in relation to paleogeographic reconstructions, *Earth Planet. Sci. Lett.*, 68, 459–470, doi:10.1016/0012-821X(84)90130-4.
- Moorbath, S., P. N. Taylor, and R. Goodwin (1981), Origin of granitic magma by crustal remobilization: Rb-Sr and Pb/Pb geochronology and isotope geochemistry of the late Archean Qôrq Granite Complex of southern west Greenland, *Geochim. Cosmochim. Acta*, 45(7), 1051–1060, doi:10.1016/0016-7037(81)90131-9.
- Moore, D. M., and R. C. Reynolds (1989), *X-Ray Diffraction and the Identification and Analysis of Clay Minerals*, 332 pp., Oxford Univ. Press, Oxford, U. K.
- O'Nions, R. K., P. J. Hamilton, and N. M. Evensen (1977), Variations in $^{143}\text{Nd}/^{144}\text{Nd}$ and $^{87}\text{Sr}/^{86}\text{Sr}$ ratios in oceanic basalts, *Earth Planet. Sci. Lett.*, 34, 13–22, doi:10.1016/0012-821X(77)90100-5.
- Oppo, D. W., J. F. McManus, and J. L. Cullen (2003), Deepwater variability in the Holocene epoch, *Nature*, 422, 277–278, doi:10.1038/422277b.

- Palmer, M. R., and H. Elderfield (1985), Variations in the Nd isotopic composition of foraminifera from Atlantic Ocean sediments, *Earth Planet. Sci. Lett.*, *73*, 299–305, doi:10.1016/0012-821X(85)90078-0.
- Patchett, P. J., and D. Bridgewater (1984), Origin of continental crust of 1.9–1.7 Ga age defined by Nd isotopes in the Ketilidian terrain of South Greenland, *Contrib. Mineral. Petrol.*, *87*, 311–318, doi:10.1007/BF00381287.
- Piotrowski, A. M., S. L. Goldstein, S. R. Hemming, and R. G. Fairbanks (2005), Temporal relationships of carbon cycle and ocean circulation at glacial boundaries, *Science*, *307*, 1933–1938, doi:10.1126/science.1104883.
- Praetorius, S. K., J. F. McManus, D. W. Oppo, and W. B. Curry (2008), Episodic reductions in bottom-water currents since the last ice age, *Nat. Geosci.*, *1*, 449–452, doi:10.1038/ngeo227.
- Revel, M., M. Cremer, F. E. Grousset, and L. Labeyrie (1996), Grain-size and Sr-Nd isotopes as tracer of paleo-bottom current strength, northeast Atlantic Ocean, *Mar. Geol.*, *131*, 233–249, doi:10.1016/0025-3227(96)00005-9.
- Richard, P., N. Shimizu, and C. J. Allegre (1976), $^{143}\text{Nd}/^{146}\text{Nd}$, a natural tracer, an application to oceanic basalts, *Earth Planet. Sci. Lett.*, *31*, 269–278, doi:10.1016/0012-821X(76)90219-3.
- Rousse, S., C. Kissel, C. Laj, J. Eiriksson, and K. L. Knudsen (2006), Holocene centennial to millennial-scale climatic variability: Evidence from high-resolution magnetic analyses of the last 10 cal kyrs off North Iceland (core MD99–2275), *Earth Planet. Sci. Lett.*, *242*, 390–405, doi:10.1016/j.epsl.2005.07.030.
- Rutberg, R. L., S. R. Hemming, and S. L. Goldstein (2000), Reduced North Atlantic deep water flux to the glacial Southern Ocean inferred from neodymium isotope ratios, *Nature*, *405*, 935–938, doi:10.1038/35016049.
- Schärer, U. (1991), Rapid continental crust formation at 1.7 Ga from a reservoir with chondritic isotope signatures, eastern Labrador, *Earth Planet. Sci. Lett.*, *102*, 110–133, doi:10.1016/0012-821X(91)90002-Y.
- Schmitz, W. J., and M. S. McCartney (1993), On the North Atlantic circulation, *Rev. Geophys.*, *31*, 29–49, doi:10.1029/92RG02583.
- Shirey, S. B., and G. N. Hanson (1986), Mantle heterogeneity and crustal recycling in Archean granite-greenstone belts: Evidence from Nd isotopes and trace elements in the Rainy Lake area, Superior Province, Ontario, Canada, *Geochim. Cosmochim. Acta*, *50*(12), 2631–2651, doi:10.1016/0016-7037(86)90215-2.
- Solignac, S., A. de Vernal, and C. Hillaire-Marcel (2004), Holocene sea-surface conditions in the North Atlantic—Contrasted trends and regimes in the western and eastern sectors (Labrador Sea vs. Iceland Basin), *Quat. Sci. Rev.*, *23*(3–4), 319–334, doi:10.1016/j.quascirev.2003.06.003.
- Stuiver, M., and P. J. Reimer (1993), Extended ^{14}C data base and revised CALIB3.0 ^{14}C age calibration program, *Radiocarbon*, *35*, 215–230.
- Tanaka, T., et al. (2000), JNd-1: A neodymium isotopic reference in consistency with LaJolla neodymium, *Chem. Geol.*, *168*, 279–281, doi:10.1016/S0009-2541(00)00198-4.
- Taylor, P. N., S. Moorbath, R. Goodwin, and A. C. Petrykoxski (1980), Crustal contamination as an indicator of the extent of early Archean continental crust: Pb isotopic evidence from the late Archean gneisses of west Greenland, *Geochim. Cosmochim. Acta*, *44*(10), 1437–1453, doi:10.1016/0016-7037(80)90109-X.
- Taylor, P. N., F. Kalsbeek, and D. Bridgewater (1992), Discrepancies between neodymium, lead and strontium model ages from the Precambrian of southern east Greenland: Evidence for a Proterozoic granulite-facies event affecting Archean gneisses, *Chem. Geol.*, *94*, 281–291, doi:10.1016/S0009-2541(10)80030-0.
- Turon, J. L., et al. (1999), *Images V, à Bord du "Marion Dufresne", 2^e Leg du 30 Juin au 24 Juillet 1999, Rapp. Mission 99-X*, Inst. Fr. de Rech. En Terres Polaires, Brest, France.
- van der Flierdt, T., and M. Frank (2010), Neodymium isotopes in paleoceanography, *Quat. Sci. Rev.*, *29*(19–20), 2439–2441, doi:10.1016/j.quascirev.2010.07.001.
- Vance, D., A. E. Scrivner, P. Beney, M. Staubwasser, G. M. Henderson, and N. C. Slowey (2004), The use of foraminifera as a record of the past neodymium isotope composition of seawater, *Paleoceanography*, *19*, PA2009, doi:10.1029/2003PA000957.
- Vervoort, J. D., W. M. White, R. I. Thorpe, and J. M. Franklin (1993), Post-magmatic thermal activity in the Abitibi Greenstone Belt, Noranda and Matagami districts: Evidence from whole-rock Pb isotopic data, *Econ. Geol.*, *88*, 1598–1614, doi:10.2113/gsecongeo.88.6.1598.
- Walter, H. J., E. Hegner, B. Diekmann, G. Kuhn, and M. Rutgers van der Loeff (2000), Provenance and transport of terrigenous sediment in the South Atlantic Ocean and their relations to glacial and interglacial cycles: Nd and Sr isotopic evidence, *Geochim. Cosmochim. Acta*, *64*(22), 3813–3827, doi:10.1016/S0016-7037(00)00476-2.
- Wasserburg, G. J., S. B. Jacobsen, D. J. DePaolo, M. T. McCulloch, and T. Wen (1981), Precise determination of Sm/Nd ratios, Sm and Nd isotopic abundances in standard solutions, *Geochim. Cosmochim. Acta*, *45*(12), 2311–2323, doi:10.1016/0016-7037(81)90085-5.
- Weis, D., et al. (2006), High-precision isotopic characterization of USGS reference materials by TIMS and MC-ICP-MS, *Geochem. Geophys. Geosyst.*, *7*, Q08006, doi:10.1029/2006GC001283.
- Williams, K. M., J. T. Andrews, N. J. Weiner, and P. J. Mudie (1995), Late Quaternary paleoceanography of the mid- to outer continental shelf, east Greenland, *Arct. Alp. Res.*, *27*, 352–363, doi:10.2307/1552028.
- Zindler, A., S. R. Hart, F. A. Frey, and S. P. Jakobsson (1979), Nd and Sr isotope ratios and rare Earth element abundances in Reykjanes Peninsula basalts evidence for mantle heterogeneity beneath Iceland, *Earth Planet. Sci. Lett.*, *45*, 249–262, doi:10.1016/0012-821X(79)90127-4.

N. Fagel, UR Argiles, Géochimie et Environnement Sédimentaires, Université de Liège, B-4000 Liège, Belgium. (nathalie.fagel@ulg.ac.be)

N. Mattielli, Département des Sciences de la Terre et de l'Environnement, Université Libre de Bruxelles, Av. Depage 30, Bldg. D, B-1050 Brussels, Belgium. (nmattiel@ulb.ac.be)